EXPERIMENTAL STUDY OF THE EFFECTS OF WIND VELOCITY AND DIRECTION ON THE FLOW AROUND AN ISOLATED BUILDING

Reginaldo Rosa Cotto de Paula, reginaldo@ifes.edu.br
Instituto Federal do Espírito Santo, Vitória, E.S.

Marcos Sebastião de Paula Gomes,
Departamento de Engenharia Mecânica, Pontíficia Universidade Católica do Rio de Janeiro, Rio de Janeiro, R.J.

Juan Carlos Dimansk Demuner, juancarlosddemuner@hotmail.com
Ana Lúcia dos Santos Ricardo, ana_dellucia@hotmail.com
Karina Scardua Pereira, karina_scardua07@hotmail.com
Instituto Federal do Espírito Santo, Vitória, E.S., Brazil

Abstract. *In this work, wind tunnel experiments were performed to investigate the effects of wind velocity and direction on the flow field around an isolated building of complex geometry. The experiments were carried out in the neutral boundary layer using three model scale buildings with different aspect rations. For oncoming flow, two buildings orientations relative to wind, with different velocities, were considered, with incident wind in the short and long faces of the buildings. The visualization during the experiments was performed using smoke injection techniques. All results showed the dependence of the flow patter around the building with its aspect ration, and the wind direction and velocity.*

Keywords*: wind tunnel experiments, flow around isolated building, atmospheric boundary layer*

1. INTRODUCTION

Investigations of the flow around building are of importance for understanding the fundamental basis of their aerodynamic characteristics (Becker et al, 2002). The wind flow and turbulence in the vicinity of an isolated building govern the wind force on the building surfaces and have a significant effect on the dispersion of atmospheric pollutants.

The flow field around a single building placed in an atmospheric boundary layer is fully turbulent and very complex, with recirculation and separation on the building surfaces and a wake region behind the building. When this problem is extended to an arbitrary building configuration this complexity is clearly amplified. Several researchers have utilized field or towing tank experiments (Wright & Easom, 2003; Zhang et al., 1996; Smith, 2001) and numerical studies (Sada & Sato, 2002; Santos et al., 2009) in order to understand the turbulent flow around an isolated building. On the order hand, this problem has been studied using scale models of buildings in wind tunnel experiments due to the possibility for exploring the effect of different buildings configurations, wind pressures on building faces and wind velocity and direction (Surry, 1991).

Boreham (1986) investigated the flow in the wake of an isolated building. Wind tunnel experiments simulated a neutrally stable atmospheric condition. Two different model buildings in simple terrains were used. The first was a simple rectangular block shape structure and the second was a low L-shaped hut. The investigations used a bipolar space charge to study the dispersion of pollutants in the wake flow region. The experiments were carried out using a new type of ion detector with a fast response time of approximately 1 ms. The method showed that was capable of providing large quantities of information about this complex flow region around the building.

Higson et al., (1996) conducted experimental investigations on the flow and dispersion around an isolated building. This study dedicated particular attention to the concentration fluctuations of the tracer gas that was released upwind of the building. The results showed that the fluctuations intensities in the field experiments were larger than those measured in the wind tunnel, except in the near-wake region.

Sarkar et al., (1997) performed a flow visualization and flow measurements on the roof of the Texas Tech Building. A tuff-grid technique was used for the flow visualization in full scale. The observations of the dynamics of the separation bubble were made based upon visualization records. The shape of the separation bubble along one axis of the building has been characterized by an intermittency factor.

Cheng et al. (2002) carried out an experimental study to determine the acrosswind response and aerodynamic damping of isolated square-shaped high-rise buildings in wind tunnel. The authors used aeroelastic models of isolated square cylinders with aspect ratio H/D = 5 and 7 in boundary layer flow. Two sets of atmospheric boundary layer were generated to represent flows over open and urban terrain. Results indicated that urban terrain flow field was aerodynamically stable for the square-shaped buildings.

Tominaga et al. (2008) used the computational fluid dynamics in order to compare different revised k-ε models and large eddy simulation (LES) applied to the flow around a high-rise building model with 1:1:2 shape placed within the surface boundary layer.

The aim of this work was to investigate the major parameters that affect the flow around an isolated building, which are the ambient conditions (wind speed and direction) and building geometry (length, height, width and roof shape). The smoke injection technique was used for the visualization of the flow structure around three different buildings with shaped of single-family house.

2. WIND TUNNEL EXPERIMENTS

The experiments were performed in the neutral boundary layer wind tunnel of Ifes, Vitória, Brazil. This facility is an open-circuit wind tunnel. Its working section is 0.5 m wide, 0.5 m high and 2.0 m long. The neutral atmospheric boundary layer was modelled at the wind tunnel making use of roughness elements and turbulence generators by using Couninhan method (Counihan, 1969).

The wind speed was measured with Pitot tube connected to a micromanometer (TSI Inc DP-CALC model 5815). Figure 1 shows the vertical velocity profile of the atmospheric boundary layer in the undisturbed flow. The mean velocity, U, was normalize by the reference velocity of the free stream, U_∞, and the height was normalized by the reference height of the boundary layer, $\delta = 0.30$ m. The wind profile consisted of measurements at $x = 1.0$ m; $z = 0.50$ m and $y = 0.05$ m, 0.10 m, …, 0.40 m. The Reynolds number (Re) was based on the free stream velocity and the model building dimensions.

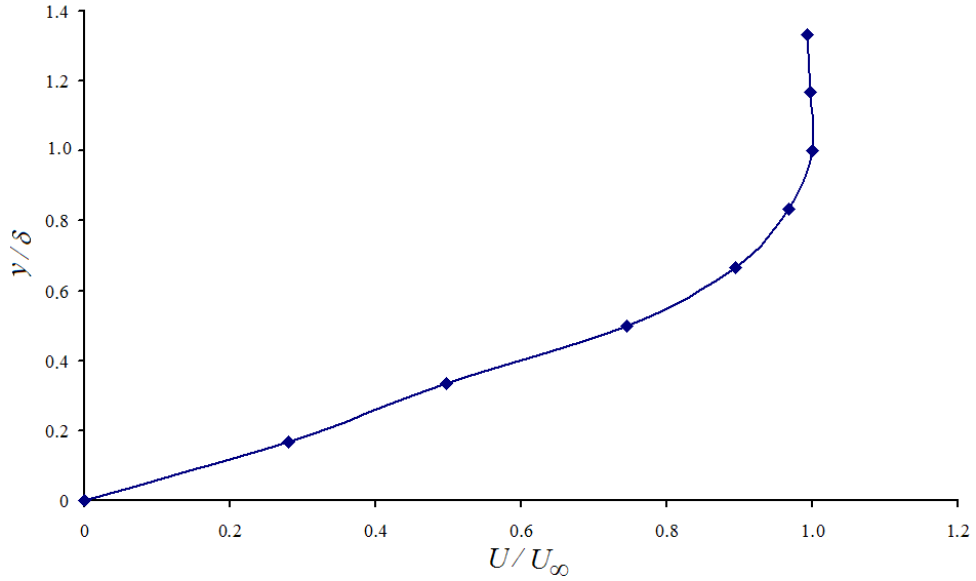

Figure 1. Typical atmospheric boundary layer vertical profiles of the mean wind in the wind tunnel.

Three wood model buildings were constructed in order to represent a single-family house building. The three buildings which were used in the experiments have the following aspect ratios ($AR = L/H$): $AR_1 = 1.67$ (Building 1: length: 0.15 m; weight: 0.12 m and height: 0.12m); $AR_2 = 3.33$ (Building 2: length: 0.30 m; weight: 0.12 m and height: 0.12 m) and $AR_3 = 0.83$ (Building 3: length: 0.15 m; weight: 0.12 m and height: 0.21 m). The building scale models were oriented at two incident wind in the frontal face, for case of an angle $\theta = 0^o$ and 90^o.

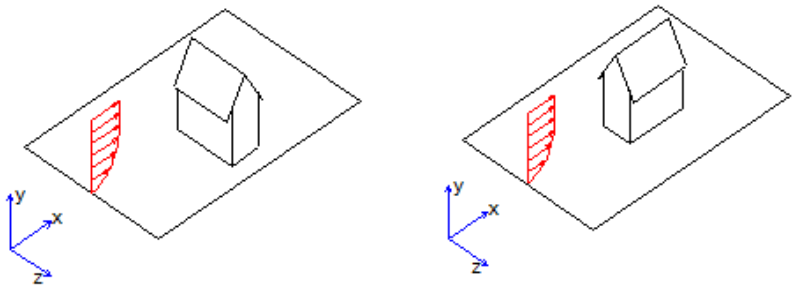

(a) (b)

Figure 2. Flow field configuration: (a) incident wind of 0^o and (b) incident wind of 90^o in the frontal face of the building.

For flow visualization in wind tunnel, in each orientation was used a smoke injection technique by using a smoke machine (Magna 900 W) with non toxic smoke fluid. A point injection was located at the center point upwind of the frontal face of the building models.

3. RESULTS AND DISCUSSIONS

3.1 – Building 1: $\theta = 0^o$ and $\theta = 90^o$ (Re = 1646)

In this section was investigated the flow visualization of the wind field around Building 1 (AR_1 = 1.67) ,for $\theta = 0^o$, $\theta = 90^o$ and Re = 1646. Figure 3 shows the side view of the flow in frontal face of Building 1 for $\theta = 0^o$. It was possible to note the formation of an eddy in front of the lower portion of the building and the separation of the flow at the roof. The flow moves out toward the recirculation region behind the building. The recirculation region is characterized by low wind speed, high turbulence intensity and low, rather uniform pressure (Hosker, 1981).

Figure 3. Side view of flow visualization for Building 1 with $\theta = 0^o$ and Re = 1646.

Figure 4 shows the side view of flow in frontal face of Building 1 for $\theta = 90^o$. The wind flow pattern showed a frontal eddy and a reattachment point at the roof. In this case it was noted a cavity zone above the roof.

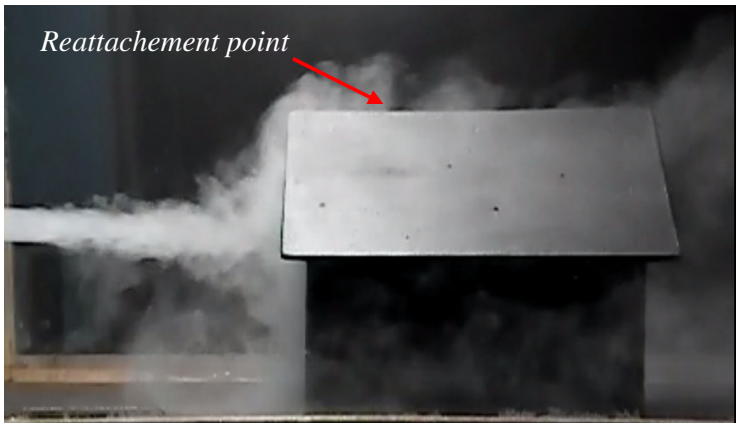

Figure 4. Side view of the flow visualization for Building 1 with $\theta = 90^o$ and Re = 1646.

3.2 – Building 2: $\theta = 0^o$ and $\theta = 90^o$ (Re = 1646)

In this section was investigated the results of flow visualization technique of the wind field around Building 2 (AR_2 = 3.33) ,for $\theta = 0^o$, $\theta = 90^o$ e and Re = 1646. Figure 5 shows the side view of flow in frontal face of Building 2 for $\theta = 0^o$. It was possible to note the formation of an eddy in front of the lower portion of the building, the flow separation at the roof and a great recirculation zone behind the roof.

Figure 5. Side view of the flow visualization for Building 2 with $\theta = 0^o$ and Re = 1646.

Figure 6 shows the side view of flow in frontal face of the Building 2 for $\theta = 90^o$. The configuration of flow field showed a frontal eddy and the flow reattached at the roof. In this case it was noted a cavity zone above the roof.

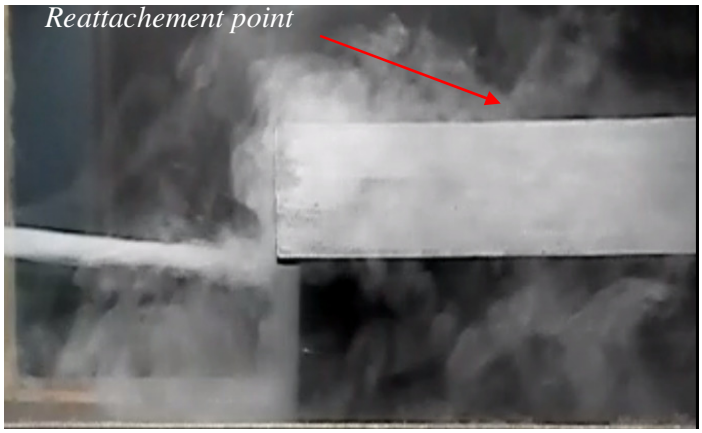

Figure 6. Side view of the flow visualization for Building 1 with $\theta = 90^o$ and Re = 1646.

3.3 – Building 3: $\theta = 0^o$ and $\theta = 90^o$ (Re = 1646)

In this section it was investigated the flow visualization of the wind field around Building 3 (AR_3 =0.83), for $\theta = 0^o$, $\theta = 90^o$ e and Re = 1646. Figure 7 shows the side view of the flow in windward face of Building 3 for $\theta = 0^o$. In this case it was noted the formation of a large eddy in frontal face of the building.

Figure 7. Side view of the flow visualization for Building 3 with $\theta = 0^o$ and Re = 1646.

Figure 8 shows the side view of flow in frontal face of Building 3 for $\theta = 90^o$. The configuration of flow field showed the formation of a standing eddy in frontal surface of building. Behind the building, it was possible to note a large cavity zone.

Figure 8. Side view of flow visualization for Building 3 with $\theta = 90^o$ and Re = 1646.

3.4 – Building 1: $\theta = 0^o$ and $\theta = 90^o$ (Re = 6055)

Figures 9 and 10 show the results of flow visualization of the velocity field in frontal face of Building 1, respectively, for $\theta = 0^o$ and $\theta = 90^o$.

Figure 9. Side view of flow visualization for Building 1 with $\theta = 0^o$ and Re = 6055.

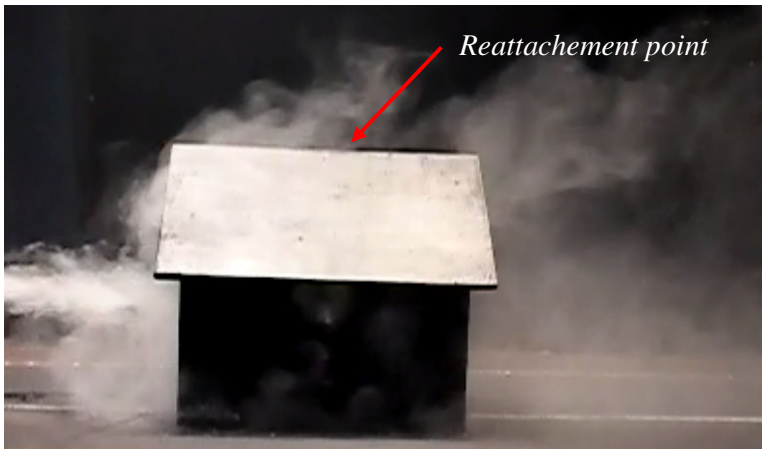

Figure 10. Side view of flow visualization for Building 1 with $\theta = 90^o$ and Re = 6055.

3.5 – Building 2: $\theta = 0^o$ and $\theta = 90^o$ (Re = 6055)

Figures 11 and 12 show the results of the flow visualization of the velocity field in the frontal face of the Building 2, respectively, for $\theta = 0^o$ and $\theta = 90^o$.

Figure 11. Side view of the flow visualization for Building 2 with $\theta = 0^o$ and Re = 6055.

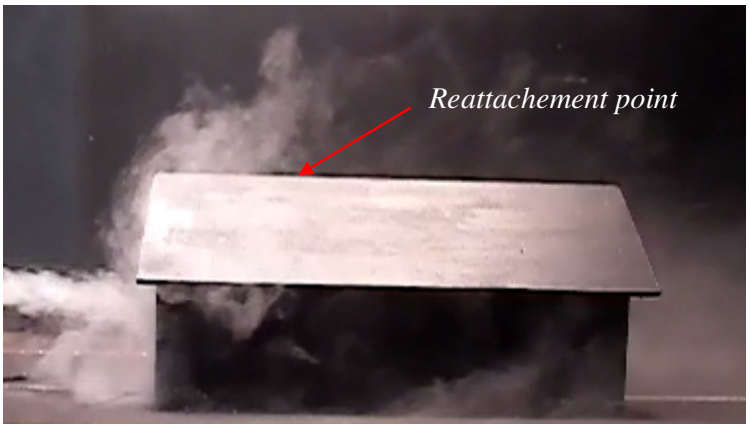

Figure 12. Side view of the flow visualization for Building 2 with $\theta = 90^o$ and Re = 6055.

3.6 – Building 3: $\theta = 0^o$ and $\theta = 90^o$ (Re = 6055)

Figures 13 and 14 show the results of flow visualization of the velocity field in frontal face of Building 3, respectively, for $\theta = 0^o$ and $\theta = 90^o$.

Figure 13. Side view of flow visualization for Building 3 with $\theta = 0^o$ and Re = 6055.

Figure 14. Side view of flow visualization for Building 3 with $\theta = 90^o$ and Re = 6055.

3.7 – Flow visualization for Re = 16876

Figures 15, 16 and 17 show the results of flow visualization of the velocity field in frontal face of Buildings 1, 2 and 3 for $\theta = 0^o$ and Re = 16876.

Figure 15. Side view of flow visualization for Building 1 with $\theta = 0^o$ and Re = 16876.

Figure 16. Side view of flow visualization for Building 2 with $\theta = 0^o$ and Re = 16876.

Figure 17. Side view of flow visualization for Building 3 with $\theta = 0^o$ and Re = 16876.

Figures 18, 19 and 20 show the results of flow visualization of the velocity field in frontal face of Buildings 1, 2 and 3 for $\theta = 90^o$ and Re = 16876.

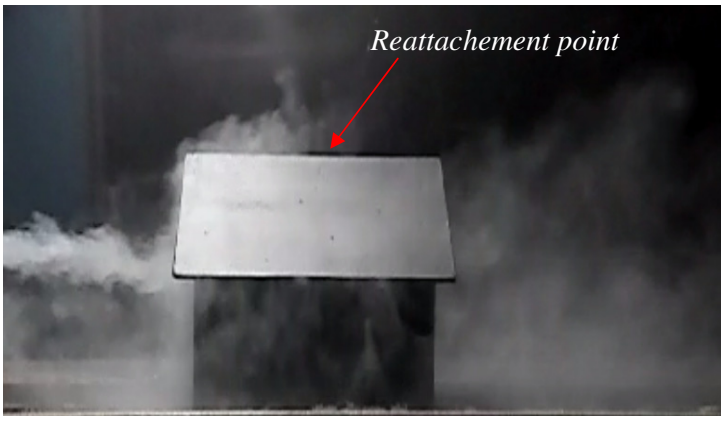

Figure 18. Side view of flow visualization for Building 1 with $\theta = 90^o$ and Re = 16876.

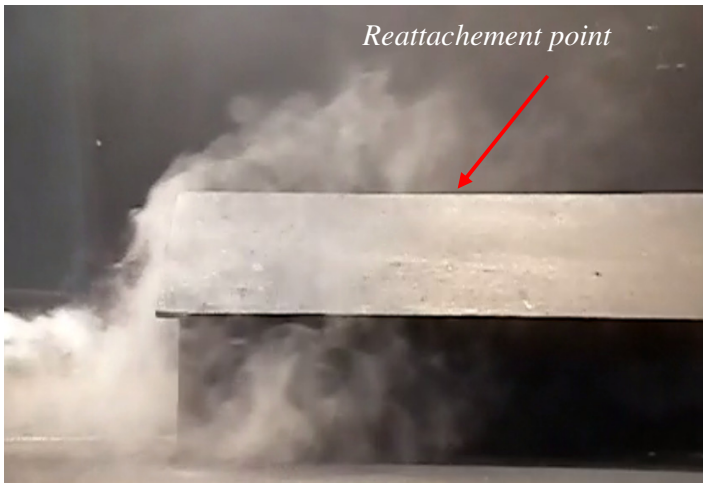

Figure 19. Side view of flow visualization for Building 2 with $\theta = 90^o$ and Re = 16876.

Figure 20. Side view of flow visualization for Building 3 with θ = 90° and Re = 16876.

Tables 1 and 2 show the experimental results of standing eddy length at frontal face of building and the recirculation length of the near wake region behind the obstacle, respectively. These parameters were analyzed for different Reynolds numbers and incident wind angles. A comparison among the obtained experimental results showed that the wind direction and wind velocity influences the field flow around the building.

Table 1. Experimental results of standing eddy length on the face frontal of building for all Re and angles of the incident wind.

	Re =1646					
	RA_1		RA_2		RA_3	
Length (m)	θ = 0°	θ = 90°	θ = 0°	θ = 90°	θ = 0°	θ = 90°
x_{eddy}	0.073	0.072	0.08	0.078	0.082	0.081
	Re = 6055					
	RA_1		RA_2		RA_3	
	θ = 0°	θ = 90°	θ = 0°	θ = 90°	θ = 0°	θ = 90°
x_{eddy}	0.072	0.069	0.084	0.065	0.083	0.085
	Re = 16876					
	RA_1		RA_2		RA_3	
	θ = 0°	θ = 90°	θ = 0°	θ = 90°	θ = 0°	θ = 90°
x_{eddy}	0.062	0.085	0.078	0.053	0.083	0.079

Table 2. Experimental results of length of the near wake region behind the building for all Re and angles of the incident wind.

	Re =1646					
	RA_1		RA_2		RA_3	
Length (m)	θ = 0°	θ = 90°	θ = 0°	θ = 90°	θ = 0°	θ = 90°
x_{wake}	0.25	0.21	0.23	0.18	0.28	0.19
	Re = 6055					
	RA_1		RA_2		RA_3	
	θ = 0°	θ = 90°	θ = 0°	θ = 90°	θ = 0°	θ = 90°
x_{wake}	0.21	0.19	0.34	0.19	0.25	0.18
	Re = 16876					
	RA_1		RA_2		RA_3	
	θ = 0°	θ = 90°	θ = 0°	θ = 90°	θ = 0°	θ = 90°
x_{wake}	0.19	0.12	0.24	0.18	0.21	0.19

5. CONCLUSIONS

The flow field in the vicinity of an isolated building with complex geometry had been studied experimentally in wind tunnel. The flow was visualized experimentally by using a smoke injection technique. Several flow regimes were found in the present work. A standing vortex was formed in the windward face of building in all experiments.

It was observed the recirculation zones behind the back faces in all experiments. The length of recirculation zone behind building for angle 0^o was greater than for angle 90^o. When the building scale models were oriented at incident wind in the frontal face with $\theta = 0^o$ was observed the separation of flow at the roof. In the case of building orientation at incident wind $\theta = 90^o$ was observed the reattachement point in the roof of building. There were distinct differences in the flow patterns in the vicinity of building due to building dimensions, velocity and incident wind. Wind tunnel studies have showed that the formation of standing eddy and recirculation region behind the obstacle respond to changes in the building orientation.

In the future it is planned to extend the physical modelling to simulate the transport and dispersion of atmospheric pollutants around buildings by using wind tunnel experiments.

6. ACKNOWLEDGEMENTS

We tank the Electrical Engineering Department of Ifes, Vitória for help with the wind tunnel facility. This research was partially supported by FACITEC/PMV – Municipal Research Council for Science and Technology of Vitória, ES/Brazil.

7. REFERENCES

Boreham, B.W. ,1986. "Preliminary wind tunnel investigation of the dispersion of pollutant particles in model building wake flows using bipolar space charge", Atmospheric Environment, Vol. 20, pp. 1523-1536.

Cheng, C.M.; Lu, P.C. and Tsai, M.S., 2002. "Acrosswind aerodynamic damping of isolated square-shaped buildings", Journal of Wind Engineering and Industrial Aerodynamics, Vol. 90, pp. 1743-1756.

Counihan, J., 1969. "An Improved Method of Simulating an Atmospheric Boundary Layer in a Wind Tunnel", Atmospheric Environment, Vol. 3, pp. 197-214.

Higson, H.L.; Griffiths, R.F.; Jones, C.D. and Hall, D.J., 1996. "Flow and dispersion around an isolated building", Atmospheric Environment, Vol. 30, pp. 2859-2870.

Hosker, Jr., R.P., 1981, "Methods for estimating wake flow and effluent dispersion near simple block-like building", NOOA, National Oceanic and Atmospheric Administration, NOAA Technical Memorandum ERL ARL-108.

Sarkar, P.P., Zhao, Z. and Mehta, K.C., 1997, "Flow visualization and measurement on the roof of the Texas Building", Journal of Wind Engineering and Industrial Aerodynamics, Vols. 69-71, pp. 597-606.

Sada, K. and Sato, A., 2002, "Numerical calculation of flow and stack-gas concentration fluctuation around cubical building", Atmospheric Environment, Vol. 36, pp. 5527-5534.

Santos, J.M., Reis Jr., N.C., Goulart, E.V. and Mavroidis, 2009, "Numerical simulation of flow and dispersion around an isolated cubical building: The effect of the atmospheric stratification", Atmospheric Environment, Vol. 43, pp. 5484-5492.

Smith, W.S., Reisner, J.M. and Kao, C.Y.J., 2001, "Simulations of around a cubical building: comparison with towing-tank data and assessment of radiatively induced thermal effects", Atmospheric Environment, Vol. 35, pp. 3811-382.

Surry, D., 1991, "Pressure measurements on the Texas Tech Building", Journal of Wind Engineering and Industrial Aerodynamics, Vol. 38, pp. 235-247.

Tominaga, Y., Mochida, A, Murakami, S. and Sawaki, S., 2008. "Comparison of various revised k–e models and LES applied to flow around a high-rise building model with 1:1:2 shape placed within the surface boundary layer", Journal of Wind Engineering and Industrial Aerodynamics, Vol. 96, pp. 389-411.

Zhang, Y.Q., Ayra, S.P. and Snyder, W.H., 1996, "A comparison of numerical and physical modeling of stable atmospheric flow and dispersion around a cubical building", Atmospheric Environment, Vol. 30, pp. 1327-1345.

Wright, N.G. and Easom, G.J., 2003, "Non-linear k–ε turbulence model results for flow over a building at full-scale", Applied Mathematical Modelling, Vol. 27, pp. 1013-1033.

8. RESPONSIBILITY NOTICE

The authors are the only responsible for the printed material included in this paper.